Available online at www.sciencedirect.com
SCIENCE DIRECT®
International Journal of Heat and Mass Transfer 47 (2004) 3375–3385
International Journal of HEAT and MASS TRANSFER
www.elsevier.com/locate/ijhmt

Heat transfer model for evaporation in microchannels. Part I: presentation of the model

J.R. Thome [a,*], V. Dupont [a], A.M. Jacobi [b]

[a] Laboratory of Heat and Mass Transfer (LTCM), Faculty of Engineering Science, Swiss Federal Institute of Technology Lausanne (EPFL), Lausanne CH-1015, Switzerland

[b] Department of Mechanical and Industrial Engineering, University of Illinois at Urbana, Champaign, Urbana 61801, IL, USA

Received 15 September 2003; received in revised form 19 January 2004
Available online 20 March 2004

Abstract

A *three-zone* flow boiling model is proposed to describe evaporation of elongated bubbles in microchannels. The heat transfer model describes the transient variation in local heat transfer coefficient during the sequential and cyclic passage of (i) a liquid slug, (ii) an evaporating elongated bubble and (iii) a vapor slug. A time-averaged local heat transfer coefficient is thus obtained. The new model illustrates the importance of the strong cyclic variation in the heat transfer coefficient and the strong dependency of heat transfer on the bubble frequency, the minimum liquid film thickness at dryout and the liquid film formation thickness.

1. Introduction

There is a growing number of experimental studies on two-phase flow and evaporation heat transfer in microchannels. A brief summary of research on evaporation in microchannels is presented here, a topic recently reviewed at length by Thome [1], Thome et al. [2], Kandlikar [3] and Bergles et al. [4]. These reviews addressed the topics of the threshold from macroscale to microscale heat transfer, two-phase flow regimes, flow boiling heat transfer results for microchannels, heat transfer mechanisms in microchannels and flow boiling prediction methods for microchannels. In contrast to macroscale evaporation, flow boiling heat transfer coefficients in microchannels have been shown experimentally to be nearly exclusively dependent on heat flux and saturation pressure while only slightly dependent on mass velocity and vapor quality. Applying macroscale ideas to the microscale, many experimental studies have concluded that *nucleate boiling* controls microchannel evaporation with a negligible convective evaporation contribution. Instead, a recent two-zone heat transfer model proposed by Jacobi and Thome [5] demonstrated that *transient evaporation of the thin liquid films surrounding elongated bubbles* is the dominant heat transfer mechanism, not nucleate boiling. Newer experimental studies have further shown that there is in fact some effect of mass velocity and vapor quality on heat transfer when covering a broader range of test conditions, including a sharp peak in the heat transfer coefficient at low vapor qualities in some cases, refer to [6–8]. Furthermore, it was concluded that macroscale models are not realistic for predicting flowing boiling coefficients in microchannels since they are based on the nucleate boiling and convective evaporation mechanisms rather than transient thin film evaporation, viz. just because an evaporation process is heat flux dependent does not mean it is nucleate boiling controlled.

As phase-change heat transfer phenomena in microscale show distinct differences from macroscale behavior, only part of the available knowledge about macroscale heat transfer can be transferred to the microscale. Several arbitrary classifications for the

* Corresponding author. Tel.: +41-21-693-5981; fax: +41-21-693-5960.
E-mail address: john.thome@epfl.ch (J.R. Thome).

0017-9310/$ - see front matter © 2004 Elsevier Ltd. All rights reserved.
doi:10.1016/j.ijheatmasstransfer.2004.01.006

Nomenclature

Bo	Bond number (dimensionless)
C_{δ_0}	correcting factor on the initial film thickness (dimensionless)
c_p	specific heat ($J\,kg^{-1}\,K^{-1}$)
d	diameter (m)
f	pair frequency (Hz)
G	mass velocity ($kg\,m^{-2}\,s^{-1}$)
h	heat transfer coefficient ($W\,m^{-2}\,K^{-1}$)
Ja	Jacob number (dimensionless)
L	length (m)
m	mass (kg)
$\dot{m}$	mass flow rate ($kg\,s^{-1}$)
Nu	Nusselt number (dimensionless)
P	pressure (Pa)
Pr	Prandtl number (dimensionless)
q	heat flux ($W\,m^{-2}$)
r	bubble radius (m)
R	internal radius of the tube (m)
Re	Reynolds number (dimensionless)
t	time (s)
U	velocity ($m\,s^{-1}$)
x	vapor quality
z	longitudinal abscissa (m)

Greek symbols

α	thermal diffusivity ($m^2\,s^{-1}$)
δ	liquid film thickness (m)
Δh_{lv}	latent heat of vaporization ($J\,kg^{-1}$)
ΔT_{sat}	superheat of the wall (K)
ε	cross-sectional void fraction of vapor
λ	thermal conductivity ($W\,m^{-1}\,K^{-1}$)
ν	kinematic viscosity ($m^2\,s^{-1}$)
ρ	density ($kg\,m^{-3}$)
τ	pair period (s)
σ	surface tension ($N\,m^{-1}$)
ξ	drag coefficient (dimensionless)

Subscripts

dry	dryout zone
dry film	dryout of the liquid film
end	end of the liquid film
film	liquid film between the bubble and the wall
G	probe location in Moriyama and Inoue (1996)
interface	liquid–vapor interface
lam	laminar flow
l	liquid
min	minimum
p	pair (liquid slug/bubble)
sat	saturation
total	two phases
trans	laminar-turbulent transition
v	vapor
$x = 1$	total vaporization
w	wall
0	initial

transition from macroscale to microscale heat transfer, based on the hydraulic diameter d for non-circular channels have been proposed. For example, Mehendale and Jacobi [9] recommend a size classification as follows: microchannels (1–100 μm), mesochannels (100 μm to 1 mm), macrochannels (1–mm) and conventional channels ($d > 6$ mm) while Kandlikar [3] recommends the following classification and size ranges: microchannels (50–600 μm), minichannels (600 μm to 3 mm) and conventional channels ($d > 3$ mm). Such transition criteria do not reflect the influence of channel size on the physical mechanisms. A more general definition should address the threshold where macroscale theory is no longer fully applicable with respect to the two-phase flow and heat transfer processes.

For now, this seems to suggest that the best threshold criterion is that to confined bubble flow, i.e. where bubble growth is confined by the channel such that bubbles grow in length rather than in diameter, which is referred to here as the elongated bubble regime. This is a likely condition below which macroscale heat transfer design methods become unreliable for predicting flow boiling heat transfer coefficients and two-phase flow pattern transitions; hence, this may provide a workable threshold for when to stop applying macroscale methods and to begin applying microscale design methods. Another important factor is the transition from laminar flow to turbulent flow. Essentially all macroscale prediction methods were developed from databases with turbulent flow occurring in the liquid phase, while many, but not all, microscale evaporation applications are at liquid Reynolds numbers below 2300.

While numerous types of flow patterns observations in microchannel flows are reported in the literature and several tentative flow pattern maps have been proposed, for example those by Triplett et al. [10], Serizawa and Kawara [11] and Tabatabai and Fahgri [12], additional research is required before a reliable prediction of flow pattern transition boundaries in microchannel flows is possible. For microchannel two-phase flows, since there is nearly no stratification effect and thus little orientation effect, the most important flow regimes are bubbly, elongated bubble, annular, mist and flows with partial dryout. For evaporating flows, the bubbly flow regime lifespan (that is, bubbles notably smaller than the channel size) is very short as bubbles grow to the

channel size very quickly, typically within a few centimeters of tube length or less. The dominant flow regime is apparently the elongated bubble flow regime followed by the annular flow regime. As will be seen here, cyclical partial dryout is also possible in the elongated bubble regime in microchannels.

In the present study, a *three-zone* flow boiling model for evaporation of elongated bubbles in microchannels is presented that qualitatively and quantitatively attempts to describe all the observed heat transfer trends noted above (including the sharp peak in the heat transfer coefficient at low vapor qualities, which is shown by the present model to be caused by the local onset of dryout at the end of elongated bubbles). The turbulent versus laminar flow question is accounted for in the present model through heat transfer modeling in the liquid and vapor slugs, which is based on their local two-phase velocity and respective Reynolds numbers. An example of the microscale elongated bubble under consideration in this work is shown in Fig. 1.

Regarding applications, micro-heat exchangers, microcooling assemblies and thermal systems implementing such devices, referred to as *micro-thermal-mechanical systems* (MTMS) as opposed to *micro-electronic-mechanical-systems* (MEMS), are rapidly advancing to ever smaller sizes. These are used as micro-cooling elements for electronic components, portable computer chips, radar and aerospace avionics components, and micro-chemical reactors. In addition to single-phase cooling applications, numerous two-phase (evaporation) cooling applications are being identified, and current implementations are pursued without the benefit of thermal design methods. Such heuristic design methods are expensive, because they rely on extensive testing. In fact, what can now be fabricated, either by micromachining of silicon wafers or micro-extrusion of aluminum elements, has vastly outpaced what can be thermally modeled. Moreover, while circular channels are the norm for macroscale evaporation processes, at the microscale non-circular channels are more common. For now, we limit our attention to channels with circular cross-sections. For general reviews on microchannel heat transfer for single-phase and two-phase flows, refer also to [9,13].

2. Previous two-zone evaporation model

It is useful to review the previous two-zone heat transfer model of Jacobi and Thome [5]. They assumed a simplified physical description of the flow and proposed an analytical model to describe evaporation in microchannels in the elongated bubble flow regime, concentrating on the transient thin film evaporation mechanism in the liquid films trapped between the wall and passing bubbles. The frequency of the bubbles was obtained from the successive nucleation and growth of bubbles across the flow channel and their subsequent departure. The bubbles then flowed downstream and elongated during their growth, with the vapor provided by thin film evaporation of the liquid film trapped between the bubble and the heated channel. This scenario has been experimentally observed during the nucleation of water from an artificial cavity [14]. Hence, as the liquid in the slug is entrained into the film and the film evaporates, the length of the liquid slug decreases and the length of the bubble increases. The local liquid film thickness decreases with time as transient thin film evaporation progresses, until the next liquid slug arrives (no dryout of the film was considered). In their two-zone model, the heat transfer to the laminar flow of the liquid slug zone was assumed to be negligible compared to heat transfer to the elongated bubble zone. Thus their model was effectively reduced to one zone with heat transfer, followed by another zone without heat transfer. To implement their model for a particular microchannel diameter, a nucleation radius had to be assumed to obtain the nucleation superheat, which was then used to calculate the time it took for a bubble in a superheated liquid to grow to the channel size and depart, giving an estimate of the bubble formation frequency. Furthermore, a value for the liquid film thickness at its formation had to be chosen as no method was available to predict its value. Parametric studies showed that the

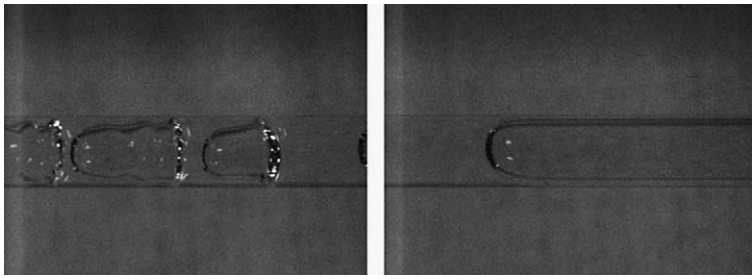

Fig. 1. Video images of elongated bubble flow (adiabatic, air–water) in a glass tube of 0.8 mm diameter, obtained with a high-resolution video camera.

model predicted several independent experimental sets described earlier quite well, when they assumed that the film thicknesses were on the order of 10–20 μm for channels 2.5 mm in size. That earlier model met its objective of proving the thin film evaporation mechanism was controlling and not nucleate boiling; however, this simple model needs to be further refined in order to more realistically and completely describe the physics and to eliminate the need for two arbitrarily adjusted parameters.

3. Three-zone evaporation model

This model is formulated to predict the local dynamic heat transfer coefficient and the local time-averaged heat transfer coefficient at a fixed location along a microchannel during flow and evaporation of an elongated bubble at a constant, uniform heat flux boundary condition. The local vapor quality, heat flux, microchannel internal diameter, mass flow rate and fluid physical properties at the local saturation pressure are input parameters for the model. The objective of the present model is to present the simplest formulation that describes the thermal process without compromising its accuracy or the basic physics of the process.

3.1. Description of the three-zone heat transfer model

Bubbles are assumed to nucleate and quickly grow to the channel size upstream such that successive elongated bubbles are formed that are confined radially by the tube wall and grow in length, trapping a thin film of liquid between the bubble and the inner tube wall. The thickness of this film plays an important role in heat transfer. At a fixed location, the process proceeds as follows: (i) a liquid slug passes (without any entrained vapor bubbles, contrary to macroscale flows), (ii) an elongated bubble passes (whose liquid film is formed from liquid removed from the liquid slug), and (iii) if the thin evaporating film of the bubble dries out before the arrival of the next liquid slug, then a vapor slug passes. The cycle then repeats itself upon arrival of the next liquid slug. Thus, either a liquid slug and elongated bubble *pair* or a liquid slug, elongated bubble and vapor slug *triplet* pass this fixed point at a frequency that is a function of the formation rate of bubbles upstream. Fig. 2(a) shows a

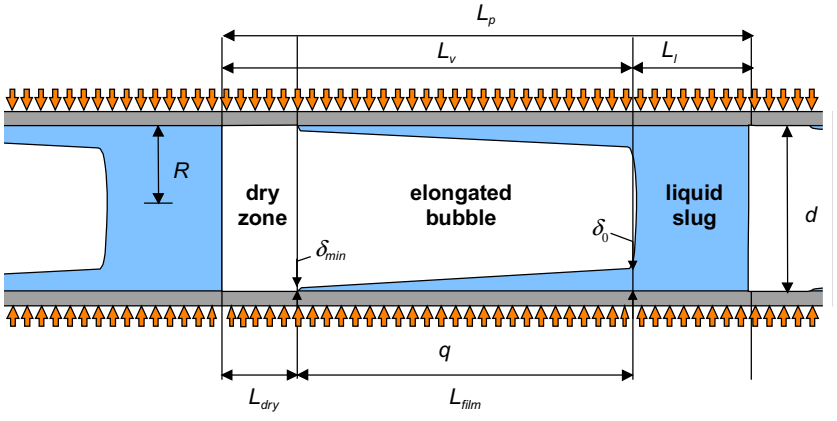

(a)

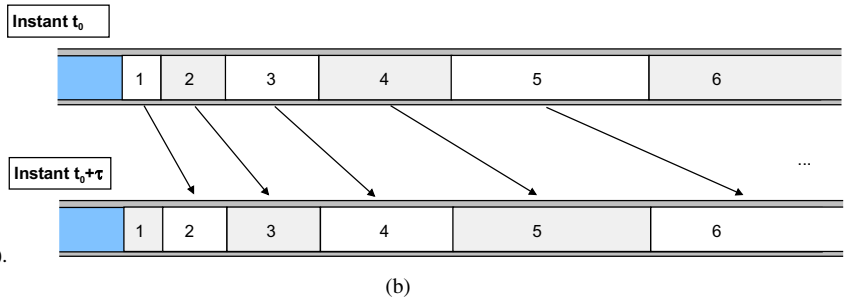

(2001).

(b)

Fig. 2. Three-zone heat transfer model for elongated bubble flow regime in microchannels: (a) diagram illustrating a triplet comprised of a liquid slug, an elongated bubble and a vapor slug; (b) tracking of a *group* of triplets with formation of new triplet at time intervals of τ.

representation of the process with a dry zone, i.e. a three-zone model. L_p is the total length of the pair or triplet, L_l is the length of the liquid slug, L_v is the length of the bubble including the length of the vapor slug with a dry wall zone L_{dry} and L_{film} is the length of the liquid film trapped by the bubble. The internal radius and diameter of the tube are R and d while δ_0 and δ_{min} are the thicknesses of the liquid film trapped between the elongated bubble and the channel wall at its formation and at dry out. The evolution of successive bubbles is shown in Fig. 2(b).

In brief, the heat transfer model is formulated as follows. In the absence of a void fraction model validated for two-phase elongated bubble flow in microchannels, the homogeneous model of two-phase flow is used to obtain the void fraction and two-phase velocity along the tube at the desired vapor quality. From the period of bubble nucleation at the inlet and the local two-phase velocity, the local length of the pair or triplet in the tube passing by this point is calculated as a function of the vapor quality, which is obtained from an energy balance from the mass flow rate and the uniform heat flux applied to the inner microchannel wall. The respective lengths of the liquid slug L_l and vapor L_v in the pair or triplet are obtained directly from the void fraction at this location. Then, from the local mean velocity of the liquid slug, the initial liquid film thickness δ_0 is calculated and dry out of the wall occurs if the film thickness reaches a predetermined value of δ_{min} before the arrival of the next liquid slug. Mean heat transfer coefficients are determined from the liquid and vapor slugs while the dynamic average value of the heat transfer coefficient of the evaporating film is determined for conduction across its varying thickness. The time-averaged heat transfer coefficient is then determined as a function of local vapor quality for one pair or triplet passing by this location of the tube.

3.2. Assumptions

The following assumptions are made in the development of the model:

1. The vapor and liquid travel at the same velocity (homogeneous flow).
2. The heat flux is uniform and constant with time along the inner wall of the microchannel.
3. All energy entering the fluid is used to vaporize liquid. Thus, the temperatures of the liquid and vapor remain at T_{sat}, i.e. neither the liquid nor the vapor is superheated.
4. The local saturation pressure is used for determining the local saturation temperature.
5. The liquid slug initially contains all liquid that flows past the nucleating bubble (at $x = 0$) until it grows to the channel diameter.
6. The liquid film remains attached to the wall. The influence of vapor shear stress on the liquid film is assumed negligible, so that it remains smooth without ripples.
7. The thickness of the film is very small with respect to the inner radius of the tube: $\delta_0 \ll R$.
8. The thermal inertia of the channel wall is neglected.

3.3. Bubble formation and frequency

The model is based on the premise that bubble nucleation occurs at the location where the fluid reaches the saturation temperature, i.e. at $x = 0$. In [5], it was assumed that such a bubble then grew in a uniformly superheated liquid to the internal diameter of the channel before departing, using the model of Plesset and Zwick [15] in the interest of the simplicity, to obtain the frequency of bubble generation. Each bubble can be envisioned as a "shutter" that divides the liquid flow into successive liquid slugs. Assuming the waiting time between successive bubbles is zero, $\tau_{wait} = 0$, then the shutter speed is given by the bubble growth rate and the internal radius of the tube R:

$$r(t) = Ja\sqrt{\frac{12\alpha_l t}{\pi}} \quad \text{with } Ja = \frac{\rho_l c_{pl}}{\rho_v \Delta h_{lv}}\Delta T_{sat} \tag{1}$$

Applying assumption 5, the bubble detaches when its radius $r = d/2$ and the period of pair generation τ is given by

$$f = 1/\tau = \left[\frac{\rho_l c_{pl}\Delta T_{sat}}{\rho_v \Delta h_{lv} R}\right]^2 \frac{12\alpha_l}{\pi} \tag{2}$$

The predicted pair frequency f for R-134a using Eqs. (1) and (2) at two superheats ($\Delta T_{sat} = 1$ and 20 K), for channel diameter ranging from 0.5 to 2 mm, ranges from over 20 to as low as 0.05 Hz, depending on the diameter of the microchannel, i.e. a variation of 400 times. In reality, shear exerted by the flow will detach the bubble before it reaches the channel diameter and thus assumption 5 decreases the pair frequency compared to early detachment. Winterton [16] proposed a relation based on the equilibrium between the drag and surface tension forces acting on a bubble of dissolved gas coming out of solution on the wall of a macrochannel in a flowing system. He assumed fully developed turbulent flow in the tube, while here the flow may be laminar. He gave two sets of equations related to the value of the contact angle (advancing and receding values). However, his method, nor apparently any other method, is available for predicting bubble departure frequencies in microchannels, which is complicated by the nucleation process. Thus, for now, f is considered as a parameter to be identified later, by comparison of the heat transfer model to experimental results. An empirical method is then proposed to predict f as a function of the process variables.

3.4. Initial conditions and basic equations

At the inlet, the mass flow rate of the liquid is that flowing past the point of bubble nucleation at the vapor quality $x = x_0$. The mass flow rate of liquid $\dot{m}_{l0}$ is given by the liquid flow rate entering the microchannel. The mass flow rate of vapor depends on the bubble formation frequency (or τ), where the vapor is treated as a separate flow injected into the liquid. The total mass flow rate thus is given by

$$\dot{m}_{\text{total}} = \dot{m}_{l0} + \frac{4}{3}\pi R^3 \frac{\rho_v}{\tau} \tag{3}$$

The corresponding total mass flux, G_{total}, is obtained by dividing by the cross-sectional area of the channel:

$$G_{\text{total}} = G + \frac{4}{3} R \frac{\rho_v}{\tau} \tag{4}$$

It is assumed that $G \approx G_{\text{total}}$. From the identification of τ, the maximum error, in this assumption, was found to range from 0.02% to 1.1% of G, except for CO_2, for which the error ranged from 0.11% to 13.5%. The case of this last fluid will be discussed in the analysis section (in the Part II of this report).

Since the mass flux of liquid is constant during the growth of the bubble, the initial length of the liquid slug L_l is determined by the frequency of bubble departure:

$$L_{l0} = \frac{G}{\rho_l}\tau \tag{5}$$

The initial length of the vapor L_v is given by the conservation of the volume of vapor, where the bubble changes from a sphere to a cylinder (the volume of the liquid film is neglected), so that

$$L_{v0} = \frac{4}{3}R \tag{6}$$

The initial length of the pair L_{p0} is thus the sum of these two lengths:

$$L_{p0} = L_{l0} + L_{v0} = \frac{G}{\rho_l}\tau + \frac{4}{3}R \tag{7}$$

At the inlet, the mean initial vapor quality x_0 is calculated from the mass flow rate of liquid and vapor during the time period τ:

$$x_0 = \frac{m_{v0}}{m_{l0} + m_{v0}} = \frac{1}{1 + \frac{3G\tau}{4\rho_v R}} \tag{8}$$

An energy balance, based on constant heat flux on the internal surface of the tube, gives the length of tube $L_{x=1}$ it takes for the liquid to be totally evaporated:

$$\begin{aligned}\dot{m}_{\text{total}}[1 - x_0]\Delta h_{lv} &= \pi R^2 G_{\text{total}}[1 - x_0]\Delta h_{lv} \\ &= 2\pi q R L_{x=1}\end{aligned} \tag{9}$$

Using Eq. (8):

$$L_{x=1} = \frac{R\Delta h_{lv}}{2q} G \tag{10}$$

Notably, the constant heat flux condition gives a linear profile of the vapor quality along the tube:

$$x(z) = \left(\frac{1 - x_0}{L_{x=1}}\right) z + x_0 \tag{11}$$

where z is the axial distance from the point of bubble nucleation at x_0.

The liquid and the vapor are assumed to travel at the same velocity, such that $U_l = U_v$, where

$$U_v = \frac{G_{\text{total}}}{\rho_v}\left(\frac{x}{\varepsilon}\right) \tag{12}$$

$$U_l = \frac{G_{\text{total}}}{\rho_l}\left(\frac{1 - x}{1 - \varepsilon}\right) \tag{13}$$

where ε is the cross-sectional void fraction.

From the equality of these two velocities, ε expressed as a function of vapor quality is

$$\varepsilon = \frac{1}{1 + \left(\frac{1-x}{x}\right)\frac{\rho_v}{\rho_l}} \tag{14}$$

The initial conditions are consistent with the homogeneous void fraction model, since the volumetric void fraction is identical to the cross-sectional void fraction for this special case.

From the expression for U_v, the velocity of the pair U_p is

$$U_p = G_{\text{total}}\left[\frac{x}{\rho_v} + \frac{1 - x}{\rho_l}\right] \tag{15}$$

Since normally $p_l \gg p_v$ in the above expression, then $U_p \approx (x/\rho_v)G_{\text{total}}$ and the pair (or triplet) velocity varies nearly linearly along the tube.

The distribution of the phases in the pair (or triplet) is represented in Fig. 2(a). Due to the periodic condition of bubble formation at the inlet, the flow inside the tube past any fixed point is also periodic in Fig. 2(b). At each location, a fixed observer sees the passage of two or three zones during the time period τ. The evolution of the heat transfer coefficient at a particular location z is shown in Fig. 3.

At each location during τ, a pair passes. It is possible to deduce the mean equivalent length of the pair at this given point:

$$L_p = U_p\tau = \tau G_{\text{total}}\left[\frac{x}{\rho_v} + \frac{1 - x}{\rho_l}\right] \tag{16}$$

This length is the apparent length of the pair measured by an observer at location z. To evaluate the residence time of a bubble t_v, at location z, the equivalent length of

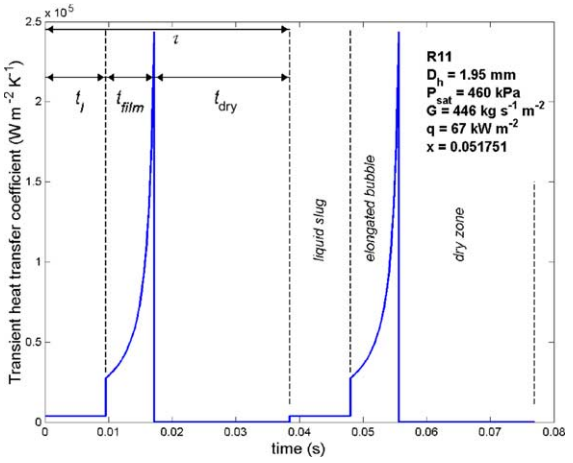

Fig. 3. Cyclic variation in heat transfer coefficient with time.

the vapor is calculated using the local mean void fraction:

$$L_{\mathrm{v}} = \varepsilon L_{\mathrm{p}} = \frac{\tau G_{\mathrm{total}}}{\rho_{\mathrm{v}}} x \tag{17}$$

so that

$$t_{\mathrm{v}} = \frac{L_{\mathrm{v}}}{U_{\mathrm{p}}} = \frac{\tau}{1 + \frac{\rho_{\mathrm{v}}}{\rho_{\mathrm{l}}} \frac{1-x}{x}} \tag{18}$$

This time t_{v} corresponds to the presence of vapor (dry-out and film zones) passing through the cross-section at location z. Similarly, to evaluate the arrival time of a bubble t_{l}, at location z, the equivalent length of the liquid slug is calculated using the local mean void fraction:

$$L_{\mathrm{l}} = (1-\varepsilon) L_{\mathrm{p}} = \frac{\tau G_{\mathrm{total}}}{\rho_{\mathrm{l}}} (1-x) \tag{19}$$

so that

$$t_{\mathrm{l}} = \frac{L_{\mathrm{l}}}{U_{\mathrm{p}}} = \frac{\tau}{1 + \frac{\rho_{\mathrm{l}}}{\rho_{\mathrm{v}}} \frac{x}{1-x}} \tag{20}$$

This time t_{l} corresponds to the presence of a liquid slug passing through the cross-section at location z.

3.5. Liquid film thickness

The initial thickness of the liquid film is a key parameter in the present model. The method for its prediction is described below.

Before addressing the thin film evaporation heat transfer model, a relation for the initial thickness of the film δ_0 layed down by the liquid slug is required. For this purpose, the Moriyama and Inoue [17] correlation, based on the Bond number Bo is used to find $\delta_0(U)$. They experimentally measured the liquid film thicknesses for bubbles growing radially between two parallel, heated, transparent plates using a technique based on video vapor front tracking and transient wall temperature analysis. The gap between the two plates ranged from $d = 100$ to 400 μm and tests were conducted with R-113. They showed that for a large superheat or bubble velocity, the viscous boundary layer controlled the formation thickness δ_0 while at a low bubble speed or small gap between the plates, the surface tension force was dominant. Their respective expressions for these two conditions are:

$$\frac{\delta_0/d}{\delta^{*0.84}} = 0.1 \quad \text{for } Bo > 2 \tag{21}$$

$$\frac{\delta_0/d}{\delta^{*0.84}} = 0.07 Bo^{0.41} \quad \text{for } Bo \leqslant 2 \tag{22}$$

where the Bond number is a function of the acceleration of the front of the bubble:

$$Bo = \frac{\rho_{\mathrm{l}} d^2}{\sigma} \frac{\mathrm{d}}{\mathrm{d}t}(U_{\mathrm{interface}}) \tag{23}$$

$$Bo \simeq \frac{\rho_{\mathrm{l}} d^2}{\sigma} \frac{U_{\mathrm{interface}}}{t_{\mathrm{G}}} \tag{24}$$

and δ^* is the dimensionless boundary layer thickness in front of the bubble:

$$\delta^* = \frac{\sqrt{\nu_{\mathrm{l}} t_{\mathrm{G}}}}{d} \tag{25}$$

In order to use a continuous relation for the expression of δ_0 over the whole range of conditions, we have applied an asymptotic expression here to calculate δ_0 using the Churchill and Usagi [18] method. As the experimental data extracted from the paper of Moriyama and Inoue [17] have some scatter, a value of $n = 8$ is selected to reasonably fit their data. Thus, the asymptotic relation is

$$\frac{\delta_0}{d} = \delta^{*0.84} \left[(0.07 Bo^{0.41})^{-8} + 0.1^{-8} \right]^{-1/8} \tag{26}$$

The main difficulty in implementing the method of Moriyama and Inoue is in estimating t_{G}, which is the time for the front of the bubble to reach a particular radius (probe site). This time is a function of the gap size d and the initial superheat (a bubble growth model is needed to complete their approach), but their experimental data can be approximated by assuming $t_{\mathrm{G}} \approx d/U$.

Another point of view is that t_{G} is associated with the thickness of the boundary layer in front of the bubble; the relation $\delta_0 \approx (\nu L/U)^{0.5}$ is used, for example, in [19] for a sliding bubble where L is a characteristical length. Addlesee and Kew [20] studied analytically the development of the film in the case of a sliding bubble under an inclined, heated plate and recommend choosing the

maximal thickness of the truncated bubble as the characteristic dimension. Thus, in our model, the diameter of the tube and the velocity of the pair ($U_{interf} \approx U_p$) are chosen to evaluate the characteristical time t_G:

$$t_G = \frac{d}{U_p} \tag{27}$$

Addlesee and Kew [20] improved their model to take into account the establishment of the liquid film. In their case, heat transfer has no influence because of the low evaporation rate due to the large thickness of the liquid film. Thus, the evolution of the film thickness was based on flow phenomena rather than heat transfer. They found that the dimensionless initial film thickness is three times the steady-state thickness given by Eq. (25); thus, this factor of 3 has been elected to modify the relation (26). In our case, evaporation is expected to be important in the variation of the film thickness; overall the expression for δ_0 was developed only from R-113 tests and the aforementioned gap range. Therefore, an empirical correction factor C_{δ_0} is introduced in Eq. (26). The value of C_{δ_0} will later be determined from a best fit to microchannel flow boiling data. Finally, the relation implemented in the present model is

$$\frac{\delta_0}{d} = C_{\delta_0}\left(3\sqrt{\frac{\nu_l}{U_p d}}\right)^{0.84}\left[\left(0.07Bo^{0.41}\right)^{-8} + 0.1^{-8}\right]^{-1/8} \tag{28}$$

This expression is used with a new Bond number definition based on the new t_G definition given by Eq. (27):

$$Bo = \frac{\rho_l d}{\sigma} U_p^2 \tag{29}$$

The predicted variation of the initial thickness of the film for R-113 at a saturation temperature of 47.2 °C in terms of the pair velocity for two microchannel diameters is provided in Fig. 4. The values were calculated using Eqs. (28) and (29). The values range from 2.1 to 6.1 μm for a pair velocity ranging from 0.5 to 1 m/s. This range of values is of the same order of magnitude as those given by Moriyama and Inoue [17] for R-113 in small spaces (0.1–0.4 mm) for the corresponding range of velocity. Fukamachi et al. [21] have measured liquid film thickness in annular or slug flow for a nitrogen–water mixture. Using an optical approach their data confirms that values below 1 μm are possible under such conditions.

The variation of liquid film thickness from its initial value of δ_0 is due only to vaporization by the heat flux q at the inner wall of the tube. For a differential length of the film Δz, all the energy transferred by conduction from the wall is used to vaporize the liquid (see Fig. 5) so that

$$Q = -\frac{dm_l}{dt}\Delta h_{lv} = -\rho_l 2\pi(R-\delta)\frac{d\delta}{dt}\Delta z \Delta h_{lv} \tag{30}$$

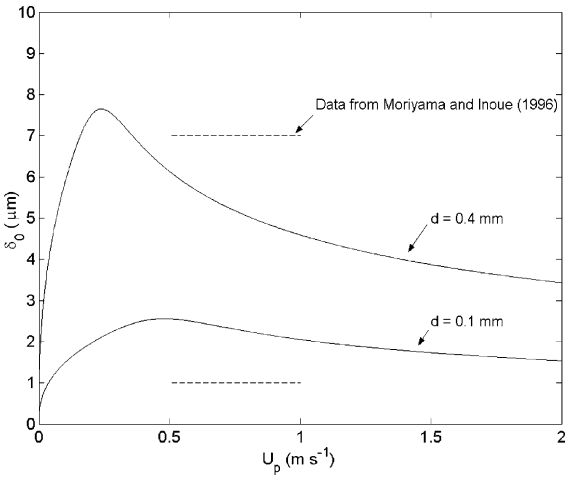

Fig. 4. Thickness of the liquid film created by the movement of the bubble versus the velocity of the front for two different tubes diameters with R-113. The maximum and minimum values of initial film thickness measured by Moriyama and Inoue (1996) are also indicated.

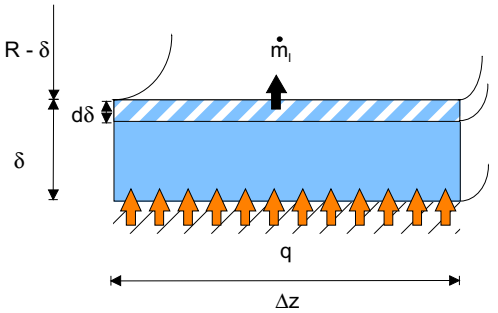

Fig. 5. Evaporation of the film.

$$Q = q(2\pi R\Delta z) \tag{31}$$

and equating these two expressions yields

$$d\delta = -\frac{q}{\rho_l \Delta h_{lv}}\frac{R}{(R-\delta)}dt \tag{32}$$

From assumption 7, $R - \delta \approx R$. The time reference is defined so that time $t = 0$ corresponds to the instant when the film is created at position z. The evolution of the thickness of the film is found by integration of Eq. (32) with the initial condition $\delta(z,0) = \delta_0(z)$ so that

$$\delta(z,t) = \delta_0(z) - \frac{q}{\rho_l \Delta h_{lv}}t \tag{33}$$

From this relation, one can express the maximum duration of the existence of the film $t_{dry\ film}$ at position z:

$$t_{dry\ film}(z) = \frac{\rho_l \Delta h_{lv}}{q}\left[\delta_0(z) - \delta_{min}\right] \tag{34}$$

The final thickness δ_{end} and residence time of the film t_{film} depend on whether or not local dry out of the film occurs. If $t_{dry\ film} > t_v$, then the next liquid slug arrives before dryout of the film occurs, so that

$$\delta_{end}(z) = \delta(z, t_v) \tag{35}$$

$$t_{film} = t_v \tag{36}$$

If $t_{dry\ film} < t_v$, then local dryout occurs, i.e. the liquid film thickness reaches the minimum feasible film thickness:

$$\delta_{end}(z) = \delta_{min} \tag{37}$$

$$t_{film} = t_{dry\ film} \tag{38}$$

Thus, the duration of the local wall dryout is

$$t_{dry} = t_v - t_{film} \tag{39}$$

The equivalent length of the dry zone at the location z is

$$L_{dry} = U_p t_{dry} \tag{40}$$

3.6. Heat transfer model

In this section, the heat transfer coefficient in each zone (liquid slug, elongated bubble and vapor slug) is analyzed. The time-averaged local heat transfer coefficient h can then be calculated for one time period τ. First, heat transfer through the thin evaporating film surrounding the elongated bubble is analyzed and then heat transfer in the liquid and vapor slugs. Note that a vapor slug is only present if the liquid film surrounding the elongated bubble reaches the minimum film thickness, at which point local, cyclical dryout occurs.

The local heat transfer coefficient in the evaporating liquid film h_{film} is

$$h_{film}(z,t) = \frac{q}{T_w - T_{sat}} \tag{41}$$

Assuming that the thin liquid film is stagnant, the local heat transfer is controlled by one-dimensional conduction across the film so that

$$h_{film}(z) = \frac{1}{t_{film}} \int_0^{t_{film}} \frac{\lambda_l}{\delta(z,t)}\, dt \tag{42}$$

$$= \frac{\lambda_l}{\delta_0 - \delta_{end}} \ln\left(\frac{\delta_0}{\delta_{end}}\right) \tag{43}$$

When $\delta \to 0$, then $h_{film} \to \infty$ and this singularity needs to be avoided. Since the liquid film will break up before approaching this limit, a criterion is required to determine the minimum possible film thickness δ_{min}. When the thickness of the film thins to the height of the surface roughness, a dry zone appears as shown in Fig. 6, the film breaks up, and a complex heat transfer process ensues that is a function of the microgeometry, contact angle, heat flux, etc. Presently δ_{min}, is assumed to be on the same order of magnitude as the surface roughness, whose value however is not specified in many existing microchannel evaporation experimental studies. Because of this complexity and the difficulty in predicting the breakup of this very thin layer, the minimum film thickness δ_{min} is one of the three adjustable parameters in the present model that will be determined from comparison of the model to experimental data and then a recommendation made.

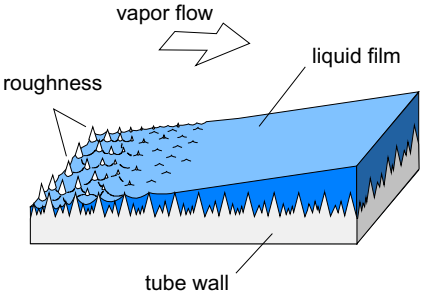

Fig. 6. Schematic of the transition from film evaporation to vapor convection in the dry zone.

For the liquid and vapor slugs (the latter is for the dry wall zone), heat transfer coefficients are calculated from their respective local Nusselt numbers and are applied to the respective "lengths" of the liquid slug L_l and dry wall zones L_{dry} passing by a given location z. The local Nusselt number at this location depends on the nature of the flow. The flow is assumed to be hydrodynamically and thermally developing.

For laminar developing flow, for which $Re \leqslant 2300$, the London and Shah correlation given by the VDI [22] is used to obtain the local Nusselt number.

$$Nu_{lam}(z) = 0.455\sqrt[3]{Pr}\sqrt{\frac{dRe}{L(z)}} \tag{44}$$

The averaged value on z gives

$$Nu_{lam,z} = 2Nu_{lam}(z) \tag{45}$$

For transition and turbulent developing flow, the Gnielinski correlation given by the VDI [22] is assumed to be valid down to $Re = 2300$ so that the local Nusselt number is

$$Nu_{trans}(z) = \frac{(\xi/8)[Re - 1000]Pr}{1 + 12.7\sqrt{\xi/8}(Pr^{2/3} - 1)}\left[1 + \frac{1}{3}\left(\frac{d}{L(z)}\right)^{2/3}\right] \tag{46}$$

where the drag coefficient ξ is

$$\xi = (1.82\log_{10} Re - 1.64)^{-2} \tag{47}$$

The averaged value on z gives

$$Nu_{\mathrm{trans},z} = \frac{(\xi/8)[Re-1000]Pr}{1+12.7\sqrt{\xi/8}(Pr^{2/3}-1)}\left[1+\left(\frac{d}{L(z)}\right)^{2/3}\right] \tag{48}$$

To obtain a continuous expression of the mean heat transfer coefficient as a function of Reynolds number, a Churchill and Usagi [18] asymptotic method has been applied, using the value $n = 4$:

$$h = [h_{\mathrm{lam}}^4 + h_{\mathrm{trans}}^4]^{1/4} = \frac{\lambda}{d}[Nu_{\mathrm{lam}}^4 + Nu_{\mathrm{trans}}^4]^{1/4} \tag{49}$$

These expressions are applicable to the liquid in the slug and to the vapor in the dry zone for their respective equivalent lengths, L_{l} and L_{dry}. Fig. 3 shows the predicted variations of h_{l} and h_{v}.

Experimentally, time-averaged local heat transfer coefficients are reported. The local, time-averaged heat transfer coefficient of a pair (or triplet) passing by location z is:

$$h(z) = \frac{t_{\mathrm{l}}}{\tau}h_{\mathrm{l}}(z) + \frac{t_{\mathrm{film}}}{\tau}h_{\mathrm{film}}(z) + \frac{t_{\mathrm{dry}}}{\tau}h_{\mathrm{v}}(z) \tag{50}$$

The new three-zone model, at this point, has three adjustable parameters, all of which are difficult to predict theoretically. They are:

- δ_{min}: the minimum thickness of the liquid film at dryout, which is related to the unknown roughness of the surface and the thermo-physical properties of the fluid;
- C_{δ_0}: the correction factor on the prediction of δ_0, the initial thickness of the liquid film given by Eq. (35), which takes into account the difference between the fluids and the geometries under investigation here from those used to establish the prediction method;
- f: the pair frequency is a complex function of the bubble formation process, which involves the channel diameter, surface roughness, nucleation process, bubble departure dynamics, subcooling in many of the experimental tests, etc.

The heat transfer model will next be compared to the experimental database to perform a parametric study to determine the optimum values of these three parameters and then generalized methods, or reasonable values, will be proposed for them in Part II.

4. Conclusions

A *three-zone* flow boiling model has been presented to describe evaporation of elongated bubbles in microchannels. The heat transfer model predicts the transient variation in local heat transfer coefficient during the cyclic passage of (i) a liquid slug, (ii) an evaporating elongated bubble and (iii) a vapor slug. The new model illustrates the importance of the strong cyclic variation in the heat transfer coefficient and the strong dependency of heat transfer on the bubble frequency, the minimum liquid film thickness at dryout and the liquid film formation thickness. Heat transfer in the thin film evaporation region is typically on the order of several times that of the liquid slug while that for the vapor slug is nearly negligible. The relative lengths of the three zones are very important as they influence the time period for each zone to pass the point of observation in each cycle and thus the value of the local time-averaged heat transfer coefficient.

Acknowledgements

A.M. Jacobi received partial support for this project as an ERCOFTAC Scientific Visitor to the Laboratory of Heat and Mass Transfer at the EPFL in Lausanne.

References

[1] J.R. Thome, Thermal phenomena in microchannels, in: Proc. 5th Int. Boiling Conf. Montego Bay, Jamaica, May 4–8, 2003.
[2] J.R. Thome, M. Groll, R. Mertz, Section 2.13.4 Microscale Heat Transfer: Boiling and Evaporation in Chapter 2.13 Heat Transfer and Fluid Flow in Microchannels, Heat Exchanger Design Update, Begell House, New York, 2.13.4.1-27, 2003.
[3] S.G. Kandlikar, Two-phase flow patterns, pressure drop and heat transfer during boiling in minichannel and microchannel flow passages of compact heat exchangers, in: Compact Heat Exchangers and Enhancement Technology for the Process Industries, Begell House, New York, 2001, pp. 319–334.
[4] A.E. Bergles, V.J.H. Lienhard, G.E. Kendall, P. Griffith, Boiling and evaporation in small diameter channels, Heat Transfer Eng. 24 (2003) 18–40.
[5] A.M. Jacobi, J.R. Thome, Heat transfer model for evaporation of elongated bubble flows in microchannels, J. Heat Transfer 124 (2002) 1131–1136.
[6] Y.Y. Yan, T.F. Lin, Evaporation heat transfer and pressure drop of refrigerant R-134a in a small pipe, Int. J. Heat Mass Transfer 41 (1998) 4183–4194.
[7] S. Lin, P.A. Kew, K. Cornwell, Two-phase heat transfer to a refrigerant in a 1 mm diameter tube, Int. J. Refrig. 24 (2001) 51–56.
[8] B. Agostini, Etude expérimentale de l'ébullition de fluide réfrigérant en convection forcée dans des minicanaux, PhD Thesis, Université Joseph Fourier, Grenoble, France, 2002.
[9] S.S. Mehendale, A.M. Jacobi, Evaporative heat transfer in mesoscale heat exchangers, ASHRAE Trans. 106 (1) (2000) 446–452.

[10] K.A. Triplett, S.M. Ghiaasiaan, S.I. Abdel-Khalik, D.L. Sadowski, Gas-liquid two-phase flow in microchannels. Part I: two-phase flow patterns, Int. J. Multiphase Flow (25) (1999) 377–394.
[11] A. Serizawa, Z. Kawara, Two-phase flow in microchannnels, 39 ETPFGM Aveiro 2001.
[12] A. Tabatabai, A. Faghri, A new two-phase flow map and transition boundary accounting for surface tension effects in horizontal miniature and micro tubes, J. Heat Transfer 1 (123) (2001) 958–968.
[13] Y. Huo, Y.S. Tian, V.V. Wadekar, T.G. Karayiannis, Review of aspects of two-phase flow and boiling heat transfer in small diameter tubes, in: Proc. 3rd Int. Conf. on Compact Heat Exchangers and Enhancement Technology for the Process Industries, Davos, Switzerland, 2001, pp. 335–346.
[14] J.Y. Lee, K. Cho, I.S. Song, C.B. Kim, S.S. Son, Microscale bubble nucleation from an artificial cavity in single microchannel, J. Heat Transfer 125 (2003) 545.
[15] M.S. Plesset, S.A. Zwick, The growth of vapour bubble in superheated liquid, J. Appl. Phys. 25 (1954) 493–500.
[16] R.H.S. Winterton, Sizes of bubbles produced by dissolved gas coming out of solution on the walls of pipes in flow systems, Chem. Eng. Sci. 27 (1972) 1223–1230.
[17] K. Moriyama, A. Inoue, Thickness of the liquid film formed by a growing bubble in a narrow gap between two horizontal plates, J. Heat Transfer 118 (1996) 132–139.
[18] S.W. Churchill, R. Usagi, A general expression for the correlation of rates of transfer and other phenomena, AIChE J. 18 (1972) 1121–1128.
[19] A.J. Addlesee, K. Cornwell, Liquid film thickness above a bubble rising under an inclined plate, Trans. IChemE 75 (1997) 663–667.
[20] A.J. Addlesee, P.A. Kew, Development of the liquid film thickness above a sliding bubble, Trans. IChemE 80 (2002) 272–277.
[21] N. Fukamachi, T. Hazuku, T. Takamasa, T. Hibiki, M. Ishii, Measurement on liquid film in microchannels using a laser focus displacement meter, in: Proc. of First ASME Int. Conf. on Microchannels and Minichannels, Rochester, New York, 2003, pp. 543–550.
[22] VDI-Wärmeatlas, Springer-Verlag, Berlin, Heidelberg, 1997.